Electrocatalysis manuscript No.
(will be inserted by the editor)

Investigating the kinetics and mechanism of organic oxidation in parallel with the oxygen evolution reaction

Asadollah Kariman · Aaron T. Marshall

Received: date / Accepted: date

Abstract In this paper, the mechanism of organic oxidation in parallel with the oxygen evolution reaction at an electrode following the "active" anode mechanism is investigated. The active anode (IrO_2-Sb_2O_5-SnO_2/Ti) was prepared via standard thermal decomposition method and 4-nitrophenol (4-NP) chosen as the model organic compound. It is firstly confirmed that this anode does follow the "active" anode mechanism, with the rate of 4-NP oxidation being dependent on the coverage adsorbed oxygen on the surface of the anode. This surface coverage can be estimated by fitting steady-state polarisation curves with a micro-kinetic model describing the oxygen evolution behaviour of the anode. This surface coverage dependent oxidation rate can only be observed at relatively low overpotentials where mass transport limitations are avoided. At high overpotentials, the rate of oxidation is completely controlled by mass transfer of 4-NP to the anode surface, with the measured and calculated rate constants agreeing closely. It is also shown that the instantaneous current efficiency can be directly calculated from the measured pseudo first order rate constant in both the kinetic and mass transport limited regimes. Using this analysis method, it was found that the instantaneous current efficiency for 4-NP oxidation is less than 100% in both regimes and only approached 100% at very low overpotentials. This finding is important as in prior literature, it is often believed that the instantaneous current efficiency of electrochemical wastewater oxidation will be 100% provided that mass transfer does not limit the process, due to an underlying assumption that the rate of organic oxidation is much larger than the OER.

Asadollah Kariman
Department of Chemical and Process Engineering, University of Canterbury, Christchurch 8140, New Zealand

Aaron T. Marshall
Department of Chemical and Process Engineering, University of Canterbury, Christchurch 8140, New Zealand
E-mail: aaron.marshall@canterbury.ac.nz

Keywords Organic oxidation · Electrochemical wastewater treatment · Oxygen Evolution Reaction · Dimensionally stablised anodes · Electrocatalysis

1 Introduction

In recent years there has been expanding attention for ecological damage by industrial contamination, and as a result much research and development into new technologies for wastewater treatment is underway [1–5]. Due to the variability of wastewater which is discharged by industrial activities [4], new advanced oxidation processes should be capable of treating toxic and non-biodegradable compounds [1,6,7].

Electrochemical wastewater treatment, where organic species are oxidized at anodes is a promising alternative to traditional processes as it has been shown to oxidise a range of compounds [5–20]. However, electrochemical oxidation has had limited penetration into industrial processes due to the high energy requirements for this process [11,12]. The presence of the oxygen evolution reaction (OER) which occurs in parallel to the oxidation of organic compounds is the main cause for high energy consumption during electrochemical wastewater treatment as this lowers the current efficiency of the process [10,11, 13]. Thus anodes with high overpotentials for the OER (known as non-active anodes [10,11]) are commonly used to increase current efficiency of organic reaction [10,11,18,21], but this in turn increases the cell potential which again leads to high energy consumption.

In order to improve the current efficiency of the organic oxidation reaction, various metal oxides have been examined [9,13,22–25]. For example, SnO_2 and Sb-doped SnO_2 have been shown to be a good anodes for electrochemical wastewater treatment as they exhibit a high overpotential for the oxygen evolution reaction and are inexpensive relative to anodes which incorporate noble metal oxide coatings [13,26]. SnO_2 based anodes are normally considered to be non-active anodes [10,11,13], where the organic oxidation mechanism involves the generation of hydroxyl radicals [9] which subsequently oxidise the organics at electrode interface and within the bulk of the electrolyte [27,28]. This generally leads to the complete oxidation of organic compounds due to the high activity and low selectivity of the hydroxyl radical for organic oxidation [9,28]. While SnO_2 or Sb-doped SnO_2 anodes exhibit good electrochemical wastewater treatment performance, by adding a small amount of IrO_2 or RuO_2 to Sb_2O_5-SnO_2 anodes, the service life and catalytic activity of the anodes can be increased dramatically [13]. However given that both IrO_2 and RuO_2 are excellent electrocatalysts for the OER, it is unclear if these additions to SnO_2 based anodes will suppress the formation of the hydroxyl radicals in favour of oxygen gas.

As the mechanism for organic oxidation is normally suggested to involve intermediates of oxygen evolution [9,29], it seems inevitable that oxygen evolution will occur in parallel with organic oxidation. The relative magnitude of these reactions will depend on both the inherent kinetics of the two reactions

and the rate of mass transfer of the organic species into the reaction zone. The latter case means even anodes with extremely poor OER kinetics, will evolve oxygen under conditions where the applied current is larger than the rate at which organics can be transported from the bulk electrolyte into the reaction zone [18,30]. For boron-doped diamond (non-active) anodes, it has been shown that it is possible to balance the organic mass transfer rate with rate of the organic oxidation reaction to achieve a current efficiency of 100% with almost complete oxidation of the organic species [17]. For non-active electrodes, this balance can be achieved as the inherent reaction rate between the generated hydroxyl radicals is both fast and independent of electrode potential. This balance however is much more difficult for active anodes. Even at applied currents above the theoretical mass transfer limited organic oxidation rate, the fraction of current which goes to the OER will be dependent of the relative kinetics of the OER and the organic oxidation reactions [29]. Clearly as the organic oxidation is mediated via the higher-oxide surface species (e.g. IrO_3) for active anodes, and as the surface coverage of these species is potential dependent, balancing reaction rate and mass transfer to achieve high current efficiencies is much more challenging.

Indeed, it conceivable that the current efficiency can be close to zero if the rate constant of organic oxidation is much smaller than that for the OER [31]. Despite this, in some cases, an assumption that organic oxidation reaction is much faster than the oxygen evolution reaction has been successfully applied in models and validated by experiment [16,32] even at electrodes which are known to by very active for oxygen evolution [25].

In the present study, we have investigated the oxidation of 4-nitrophenol (4-NP) at IrO_2-Sb_2O_5-SnO_2/Ti anodes to gain insights into the reaction mechanism and process efficiency. Firstly, given that SnO_2 is considered a non-active anode whereas IrO_2 an active anode, we have attempted to determine whether this mixed IrO_2-Sb_2O_5-SnO_2 electrode behaves as an active or non-active anode. Secondly, given that the vast amount of literature on electrochemical wastewater treatment investigates the process under mass transfer limited conditions, we have also attempted to measure the kinetics of the organic oxidation reaction in absence of any mass transfer limitations so that the dependence of reaction rate on the higher-oxide surface coverage can be established and compared to a micro-kinetic model. And finally, we develop a simple set of equations which can be used to estimate the instantaneous current efficiency from an experimentally determined rate constant.

2 Experimental

Dimensionally stabilized anodes were prepared by coating a titanium substrate with a IrO_2-Sb_2O_5-SnO_2 layer using the standard thermal decomposition technique [33]. Briefly, the titanium discs (Grade 2, diameter=45mm) were etched in concentrated HCl in an ultrasonic bath for 40 minutes, then rinsed in deionized water and isopropanol, before being dried at 105 °C. A precursor solution

was prepared by dissolving 0.16 g of $IrCl_3.3H_2O$ (99.8%, Sigma-Aldrich), 1 g of $SnCl_2$ (98%, Sigma-Aldrich) and 0.1 g of $SbCl_5$ (99.99%, Sigma-Aldrich) into 9 mL of isopropanol (99.9%, ASCC) and 1 mL of concentrated HCl (37%, Fisher chemical). The precursor solution composition was chosen to achieve the an anode coating similar to that described by Adams *et al.* [13] of 10 wt% IrO_2 and 90 wt% SnO_2-Sb_2O_5 (Sn:Sb molar ratio 16:1). Approximately 0.2 mL of this precursor solution was sprayed on the titanium disk held at 80 °C before heating at 450 °C in air for 10 minutes to oxidise the precursor. This spray / heating process was repeated five times before the final layer was annealed for 1 hour at 450 °C. The final total oxide loading was measured gravimetrically to be approximately 1 mg cm^{-2}.

The electrochemical measurements were carried out in a parallel plate electrode flow cell connected to a continuous stirred 150 mL electrolyte reservoir via a peristaltic pump (Masterflex console drive). The electrolyte was 0.5 M Na_2SO_4 (99.4%, Labserv) acidified to pH 1.75 (using concentrated sulfuric acid) with or without the addition of 4-NP (99%, BDH) and the flow rate set at 160 mL min^{-1}. The anode in this cell was the prepared IrO_2-Sb_2O_5-SnO_2/Ti electrode, the cathode was a stainless steel plate and a saturated calomel reference electrode (SCE) was placed in the electrolyte reservoir. The space between anode and cathode was 1 cm and the each of these electrodes had an exposed area of 12.56 cm^2. To account for the ohmic resistance between the anode and the reference electrode, electrochemical impedance spectroscopy was measured over a frequency range of 100 kHz to 10 mHz, with an AC amplitude of 10 mV and a DC potential of 0.6 V vs SCE. Typically, the resistance between the anode and the reference electrode was around 1 Ω, and was used to compensate the IR drop after the cyclic voltammetry and polarization measurements. A Gamry Interface 1000 potentiostat was used to control the electrochemical measurements. All potentials in this paper are referenced against the SCE unless otherwise stated.

As the mass transport behaviour within the electrochemical flow cell has a strong influence on the current efficiency of 4-NP oxidation, the diffusion layer thickness (δ) at the anode under the hydrodynamic conditions used in this work was measured using the Fe^{3+}/Fe^{2+} redox couple (5 mM $NH_4Fe(SO_4)_2$ and $FeSO_4$ in 0.5 M H_2SO_4). Briefly, a gold wire (diameter 1 mm) was embedded in an acrylic disc and used in place of the anode. Then the mass transport limiting current density for the reduction of Fe^{3+} to Fe^{2+} was measured over a range of flow rates and the diffusion thickness layer calculated from:

$$\delta = \frac{nFDC_{bulk}}{i_{lim}} \tag{1}$$

Where i_{lim} is the limiting current density (A cm^{-2}), n is the number of electrons transferred, F the Faraday constant (96485 C mol^{-1}), D is the diffusion coefficient of Fe^{3+} (5.6×10^{-6} cm^2 s^{-1}) [34], C_{bulk} is the concentration of the Fe^{3+} in the bulk of the electrolyte (mol cm^{-3}). At the typical electrolyte flow rate of 160 mL min^{-1}, this yielded a diffusion layer thickness of 95 μm.

The potentiostatic oxidation of 4-NP was conducted between 1.2 and 1.5 V vs SCE to ensure both the kinetically and mass transport limited oxidation regimes were observed. During the oxidation, electrolyte samples were taken periodically and the concentration of 4-NP determined spectroscopically using a UV/Vis spectrophotometer (UV-1600PC, VWR). Here, it was found that the absorbance peak at 319 nm was directly proportional to concentration of 4-NP between 0 and 0.15 mM in agreement with others [13]. It was also found that the 4-NP was stable (no observed changes in the UV/Vis spectra) in 0.5 M Na_2SO_4 at pH=1.75 for at least 5 weeks, indicating that any changes in the UV/Vis spectra during potentiostatic oxidation can be contributed to the electrochemical process.

3 Results and Discussion

While the anodic oxidation of organic molecules at electrodes have fairly complex reaction mechanisms, some useful insights can be gained by considering simple cases. The two most important general mechanisms for the oxidation of organics at anodes were first proposed by Comninellis [9], and are based on either "active" or "non-active" anodes. For active anodes, the oxidation of the organic is mediated by the higher-oxide (S-O, e.g. IrO_3) formed on the anode surface at potentials above the thermodynamic OER potential, whereas on non-active anodes the organic is oxidised by hydroxyl radicals generated by anode. Given that the potential for hydroxyl radical generation is 2.74 V vs NHE [35], if the anode operates at potentials much lower than this, it seems reasonable to assume that hydroxyl generation will be negligible. This is certainly consistent with IrO_2 anodes which are known to operate at low anodic potentials (IrO_2 is an excellent electrocatalyst for the OER) and have been shown not to generate significant quantities of hydroxyl radicals [9]. Furthermore, both boron-doped diamond and SnO_2 anodes are known to generate hydroxyl radicals and are typically found to have very high overpotentials for the OER. In this work, it has been found that the IrO_2-Sb_2O_5-SnO_2/Ti anode can operate the OER at a current density of 10 mA cm^{-2} with an overpotential of only 360 mV, which is consistent with others who show that additions of as low as 0.5 mol% IrO_2 to SnO_2 anodes can dramatically lower the overpotential for the OER [36]. Thus, it is assumed that the IrO_2-Sb_2O_5-SnO_2/Ti anode is unlikely to generate the hydroxyl radical and therefore will operate via the "active" anode mechanism. To ensure that the mechanism is consistent with proposed mechanisms for the OER, here it is the higher-oxide is formed via the electrochemical oxide path [37]:

$$S + H_2O \rightleftharpoons S{-}OH + H^+ + e^- \quad \text{(R1)}$$

$$S{-}OH \rightleftharpoons S{-}O + H^+ + e^- \quad \text{(R2)}$$

$$S{-}O \rightleftharpoons S + \tfrac{1}{2}\,O_2 \quad \text{(R3)}$$

Where S is a free-surface site. The higher-oxide formed in step two of the OER mechanism can form oxygen gas via reaction R3 or oxidise an organic molecule (R) via reaction R4:

$$S{-}O + R \longrightarrow S + RO \tag{R4}$$

Thus it should be expected that oxygen gas evolution will compete with the oxidation of organics within an electrochemical wastewater treatment process, when the anode potential is above 1.23 V vs RHE. However, as the thermodynamic requirements for organic oxidation are often lower than that for oxygen evolution, it is possible that oxidation of organic compounds can occur below 1.23 V vs RHE. In this work, this possibility was assessed via cyclic voltammetry.

These cyclic voltammetry measurements revealed that almost no difference between the electrochemical behaviour of the IrO_2-Sb_2O_5-SnO_2/Ti anode in 0.5 M Na_2SO_4 and 0.15 mM 4-NP in 0.5 M Na_2SO_4 solution (Fig. 1). The rather featureless voltammograms in 0.5 M Na_2SO_4 is consistent with the behaviour of IrO_2 and SnO_2 anodes prepared by thermal decomposition [13, 38] with only double-layer charging and pseudo-capacitive behaviour observed at potentials between 0.1 and 1.15 V. As the potential is swept above 1.15 V (1.29 V vs RHE), an anodic current most likely originating from oxygen evolution is observed in both electrolytes. Importantly, no evidence to suggest the anodic oxidation of 4-NP occurs between 0.1 and 1.1 V, and thus we conclude that the oxidation of 4-NP must occur at potentials high enough for oxygen evolution (*i.e.* above 1.15 V).

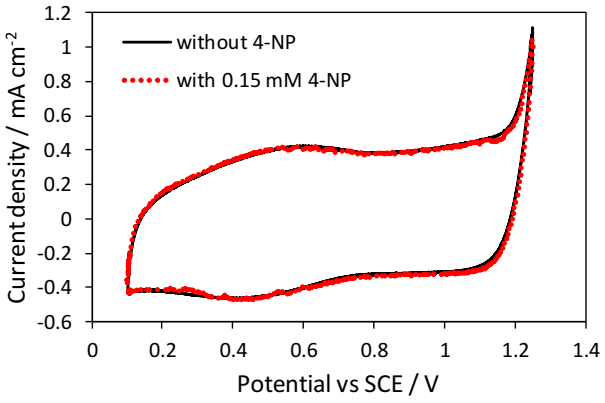

Fig. 1 Cyclic voltammetry of the IrO_2-Sb_2O_5-SnO_2/Ti electrode in 0.5 M Na_2SO_4 and in 0.5 M Na_2SO_4 containing 0.15 mM 4NP. Sweep rate = 50 mV/s, pH=1.75

At potentials above 1.2 V, the anodic oxidation of 4-NP is observed by monitoring the absorbance at 319 nm. As the potential increases from 1.2 V, the overall oxidation rate also increases until 1.3 V, after which no further

changes in the 4-NP concentration vs time behaviour was observed (Figure 2a). Clearly no further enhancements in the oxidation rate of 4-NP can be achieved above 1.3 V, suggesting either electrode kinetics or mass transport begins to limit the oxidation rate above 1.3 V. The oxidation rate is to be pseudo first order in respect to the 4-NP concentration with linear $ln(C_{bulk}/C_{(bulk,0)})$ vs time behaviour found over the entire potential range examined (Figure 2b). Assuming that the rate of the 4-NP oxidation (equation 4) is given by:

$$\frac{dC_{bulk}}{dt} = -k_4\theta_{\mathrm{O}}C_{bulk} \tag{2}$$

where k_4 is the rate constant for reaction R4, θ_{O} is the surface coverage of the higher oxide (S-O) and C_{bulk} is the concentration of 4-NP in the electrolyte bulk. This can be simplified further to be a pseudo first order reaction, if it is assumed that the surface coverage of the higher-oxide is approximately constant throughout the electrolysis time:

$$\frac{dC_{bulk}}{dt} = -k_{4,app}C_{bulk} \tag{3}$$

Where the pseudo first order reaction rate constant is $k_{4,app} = k_4\theta_{\mathrm{O}}$. As with the overall 4-NP oxidation rate, the calculated pseudo first order rate constant is clearly found to increase with potential until 1.3 V (Fig. 3). Above this potential, as no further increase in the pseudo first order rate constant occurs, any further additional current above that found at 1.3 V will be wasted in reactions other than 4-NP oxidation (most likely the oxygen evolution reaction).

To understand why the pseudo first order rate constant is potential dependent between 1.2 and 1.3 V, first the potential dependence of the higher-oxide surface coverage (θ_{O}) is examined. This can be estimated by fitting the OER behaviour of the anode (i.e. a polarisation curve in absence of 4-NP) to a micro-kinetic model of the OER following the electrochemical oxide pathway [39]. Briefly, the reaction rates for each step in the OER (R1-R3) are given by:

$$r_1 = k_1C_{\mathrm{H_2O}}\left(1-\theta_{\mathrm{OH}}-\theta_{\mathrm{O}}\right) - k_{\text{-}1}C_{\mathrm{H^+}}\theta_{\mathrm{OH}} \tag{4}$$

$$r_2 = k_2\theta_{\mathrm{OH}} - k_{\text{-}2}C_{\mathrm{H^+}}\theta_{\mathrm{O}} \tag{5}$$

$$r_3 = k_3\theta_{\mathrm{O}} - k_{\text{-}3}C_{\mathrm{O_2}}^{1/2}\left(1-\theta_{\mathrm{OH}}-\theta_{\mathrm{O}}\right) \tag{6}$$

where k_1 and $k_{\text{-}1}$ *etc.* are forward and back rate constants and C are concentrations of protons or dissolved oxygen. θ_{OH} and θ_{O} are the surface coverage of OH and O respectively.

As steps R1 and R2 are electrochemical reactions, the rate constants k_1, $k_{\text{-}1}$,k_2, and $k_{\text{-}2}$ are potential dependent as per Butler-Volmer kinetics, *e.g.*:

$$k_i = k_i^0 \exp^{\frac{\beta F}{RT}(E-E_{rev})} \tag{7}$$

$$k_{\text{-}i} = k_{\text{-}i}^0 \exp^{\frac{-(1-\beta)F}{RT}(E-E_{rev})} \tag{8}$$

where, E and E_{rev} are the anode and reversible potential for the OER respectively and β, F, R and T are the symmetry factor, Faraday constant, gas

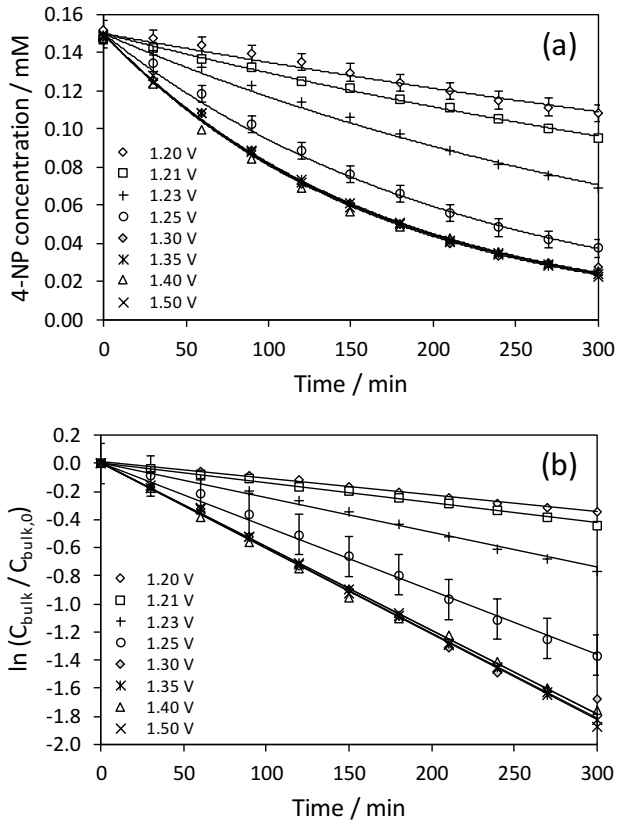

Fig. 2 Potentiostatic electrolysis of a 0.5 M Na_2SO_4 solution (pH=1.75) initially containing 0.15 mM of 4-NP. (a) Concentration (C_{bulk}) vs time, (b) first-order plot of $ln(C_{bulk}/C_{(bulk,0)})$

constant and temperature respectively. While it is often assumed that $\beta = 0.5$, as this is know to differ from 0.5 for processes involving adsorbed species [40], β is allowed to vary during the fitting procedure. From these kinetic equations, the differential equations describing the surface coverages of S-OH and S-O can be solved at steady-state to give:

$$\theta_{\mathrm{O}} = \frac{\frac{k_{\text{-}3}C_{\mathrm{O_2}}^{1/2}}{k_{\text{-}3}C_{\mathrm{O_2}}^{1/2}-k_2} - \frac{k_1 C_{\mathrm{H_2O}}}{k_1 C_{\mathrm{H_2O}}+k_{\text{-}1}C_{\mathrm{H^+}}+k_2}}{\frac{k_{\text{-}2}C_{\mathrm{H^+}}-k_1 C_{\mathrm{H_2O}}}{k_1 C_{\mathrm{H_2O}}+k_{\text{-}1}C_{\mathrm{H^+}}+k_2} - \frac{-k_{\text{-}2}C_{\mathrm{H^+}}-k_3-k_{\text{-}3}C_{\mathrm{O_2}}^{1/2}}{k_{\text{-}3}C_{\mathrm{O_2}}^{1/2}-k_2}} \tag{9}$$

$$\theta_{\mathrm{OH}} = \frac{\theta_{\mathrm{O}}\left(-k_{\text{-}2}C_{\mathrm{H^+}} - k_3 - k_{\text{-}3}C_{\mathrm{O_2}}^{1/2}\right) + k_{\text{-}3}C_{\mathrm{O_2}}^{1/2}}{k_{\text{-}3}C_{\mathrm{O_2}}^{1/2} - k_2} \tag{10}$$

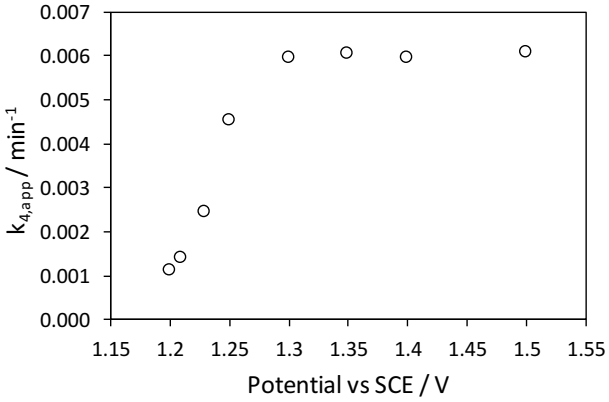

Fig. 3 The dependence of the first order rate constant ($k_{4,app}$) on applied potential at the IrO_2-Sb_2O_5-SnO_2/Ti anode. The maximum uncertainty in the calculated rate constant (95% confidence interval) was found to be 2×10^{-4} min^{-1}.

These surface coverages are used along with the rate constants to determine the reaction rates and thus the OER current density (i_{OER}) as a function of potential at steady-state:

$$i_{\mathrm{OER}} = F\,(r_1 + r_2) \tag{11}$$

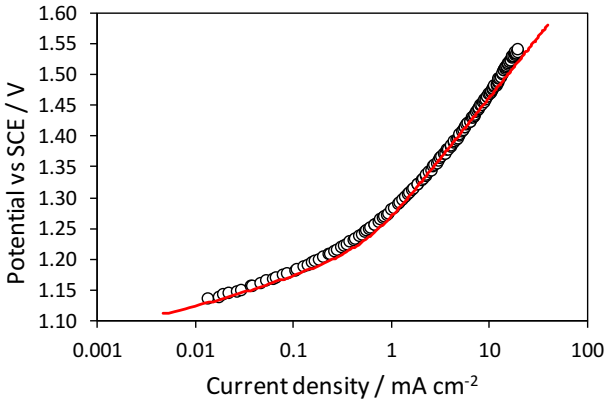

Fig. 4 Comparison between the experimentally measured (circles) and the calculated (line) oxygen evolution reaction steady-state polarisation curves in 0.5 M Na_2SO_4 at pH=1.75.

Here is it found that this kinetic model fits the experimentally determined OER polarisation curve reasonably well (Fig. 4), with the high Tafel slope ($\approx$ 140 mV) suggesting that the initial discharge of water (R1) is the rate determining step for the OER reaction on this IrO_2-Sb_2O_5-SnO_2/Ti anode. It

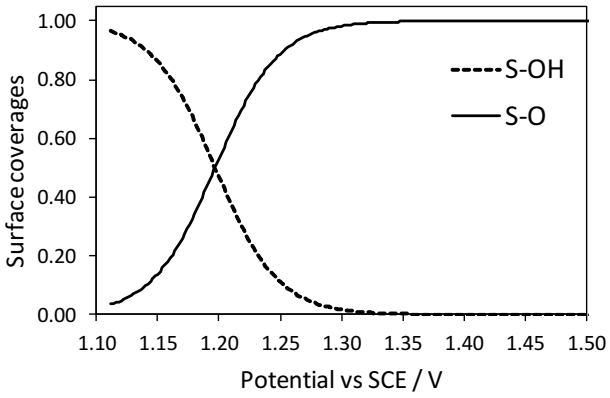

Fig. 5 Calculated surface coverages of the surface bound intermediates during the oxygen evolution reaction at pH=1.75.

is also found that the surface coverage of S-O increases from close to 0 to almost 1 between 1.1 and 1.3 V (Fig. 5). This increase in the surface coverage of S-O with potential, agrees well with the measured increase the pseudo-first order rate constant ($k_{4,app} = k_4\theta_{\mathrm{O}}$) and suggest that this is the main reason for the potential dependence in the rate constant. As the surface coverage approaches 1 above 1.3 V, it is possible that this could limit the organic oxidation reaction rate. However, as that initial step in the overall reaction mechanism is that rate limiting step, in this case it is unlikely that the apparent limit in the rate constant above 1.3 V is related to inherent kinetics. Rather it seems more likely that this limit is related to the mass transport of organic from the bulk to the electrode surface.

To investigate this hypothesis, the pseudo first order rate constant under mass transport control was determined. Given that the change in 4-NP concentration within the bulk of the electrolyte will be equal to the mass transport across the diffusion layer to the electrode surface, the change in 4-NP concentration (C_{bulk}) with time is described by:

$$\frac{dC_{bulk}}{dt} = -\frac{DA}{\delta V}\left(C_{bulk} - C_{surf}\right) \tag{12}$$

When the oxidation of 4-NP at the electrode surface is controlled by mass transfer, the surface concentration of 4-NP (C_{surf}) will be zero. With this, by comparing equations 3 and 12 , the pseudo first order rate constant under mass transport control ($k_{4,app,lim}$) can be calculated by:

$$k_{4,app,lim} = \frac{DA}{\delta V} \tag{13}$$

Using a diffusion coefficient (D) of 0.919×10^{-5} cm^2 s^{-1} [41], an experimentally determined diffusion layer thickness (δ) of 95 μm, an anode area (A) of 12.56 cm^2 and an electrolyte volume (V) of 150 mL, the pseudo first order rate

constant for a mass transport limited process ($k_{(app,lim)}$) at our hydrodynamic conditions is calculated to be 0.0056 min^{-1}. This value agrees closely with the observed limit in the measured pseudo first order rate constant (0.0060 min^{-1}, Figure 3) which confirms that the electrochemical oxidation of 4-NP is limited by mass transport at potentials above 1.3 V.

As the 4-NP oxidation rate is limited by mass transport above 1.3 V, it must be concluded that the instantaneous current efficiency for 4-NP oxidation must be below 100% and thus energy is wasted in the OER. This is well understood in the previous literature and many have developed models to estimate the instantaneous current efficiency under mass transport limiting rates [16, 25,32,42]. However, below 1.3 V, the results here suggest that the oxidation of 4-NP will not be limited by mass transport and is instead limited by the production rate of the S-O on the surface of the anode. As the 4-NP oxidation will compete with the final step of the OER reaction for these surface bound O species, it is important to estimate the instantaneous current efficiency. In previous models [16,25,32,42], it has been assumed that the organic oxidation rate is must faster than the final recombination step of the OER mechanism, which results in the prediction that in absence of any mass transport limitations, the instantaneous current efficiency will be 100%. To investigate whether this is indeed the case, here the equivalent current density going to 4-NP oxidation is estimated and compared with the actual current density measured throughout the experiment.

In order to calculate the equivalent current density going to 4-NP oxidation (i_{4NP}) the following approach was used. Firstly, this current density can be directly related to the change in 4-NP concentration by:

$$\frac{dC_{bulk}}{dt} = -\frac{i_{4NP}}{nF}\frac{A}{V} \tag{14}$$

where n represents the number of electrons which must be transferred as part of the first two steps of the OER mechanism to oxidise a 4-NP molecule. For the oxidation of 4-NP, the minimum value for n is 2 and the maximum value is 28 [43]. The logical products formed by a $n = 2$ oxidation would be 4-nitrocatechol or hydroquinone as these have been observed during solution phase oxidation [44]. However, we did not observe any development of UV/Vis absorbance peaks consistent with 4-nitrocatechol (309 and 345 nm [45]) or hydroquinone (288 nm [46]) and so it seems unlikely that these compounds are the final oxidation products from 4-NP. It is also possible that 1,4-benzoquinone could form via a $n = 4$ oxidation and we did observe small absorbance peaks around 245 nm which could be consistent with 1,4-benzoquinone [46], although we suspect that this just indicates that 1,4-benzoquinone is one of the intermediates of complete 4-NP oxidation as others have confirmed that complete oxidation of 4-NP to CO_2, H_2O and HNO_3 is possible [47]. To provide an accurate measurement of the equivalent electrons used during 4-NP oxidation either total carbon analysis or complete product identification and quantification would be required. Rather, here the maximum possible instantaneous current efficiency is determined by assuming that

the disappearance of 4-NP (as detected by UV/Vis spectroscopy) corresponds to complete oxidation ($n = 28$). Integrating equation 3 gives:

$$C_{bulk} = C_{bulk,0} \exp^{-k_{4,app}t} \tag{15}$$

and thus with equation 3:

$$\frac{dC_{bulk}}{dt} = -k_{4,app}C_{bulk,0} \exp^{-k_{4,app}t} \tag{16}$$

Using this with equation 14 then gives:

$$i_{4NP} = -\frac{k_{4,app}C_{bulk,0}nFV}{A} \exp^{-k_{4,app}t} \tag{17}$$

and then instantaneous current efficiency (ICE) for 4-NP oxidation can be determined from:

$$ICE = \frac{i_{4NP}}{i_{total}} \tag{18}$$

As expected, the calculated current density resulting in 4-NP oxidation is found to increase with potential until 1.3 V (Fig. 6) after which this current becomes limited by mass transport (or possibly reaction kinetics). Interestingly, the ICE is seen to increase in the first 30 min of 4-NP oxidation (Fig. 7) which reflects the significantly higher current observed at the start of electrolysis period. It is likely that while the 4-NP oxidation current density slowly decreases over time as the 4-NP is removed, the OER may be slightly poisoned in the first 30 minutes which decreases the kinetics of the OER, and thus improves the ICE for 4-NP oxidation. This analysis clearly shows that the ICE can be less than 100% when the 4-NP oxidation reaction is limited by kinetics rather than mass transport. This finding is important as it indicates that it cannot always be assumed that the organic oxidation reactions will be much faster than the OER when using anodes known to be active for the OER.

By integrating the current going to 4-NP oxidation over 200 minutes of oxidation and comparing this with the total charge passed during this time, the general current efficiency can be determined (Fig. 8). As expected from the ICE results, the general current efficiency is highest at the lowest anode potentials and decreases continuously with increasing anode potential. Between 1.2 and 1.3 V, the decrease in general current efficiency is due to the increasing rate of the OER kinetics relative to the kinetics of 4-NP oxidation. In this case, the OER kinetics increase faster than the kinetics of 4-NP oxidation as the final step of the OER is proportional to the square of the S-O surface coverage, whereas the kinetics of 4-NP are directly proportional to the S-O surface coverage. Above 1.3 V, the continued decrease in the general current efficiency is dominated by the limitation in the mass transport of 4-NP from the bulk of the electrolyte to the anode surface.

Based on our results, some general conclusions can be reached regarding electrochemical wastewater oxidation at oxide anodes following the active electrode mechanism. Firstly, the oxidation should always be conducted at potentials (or current densities) below where mass transport limits the oxidation

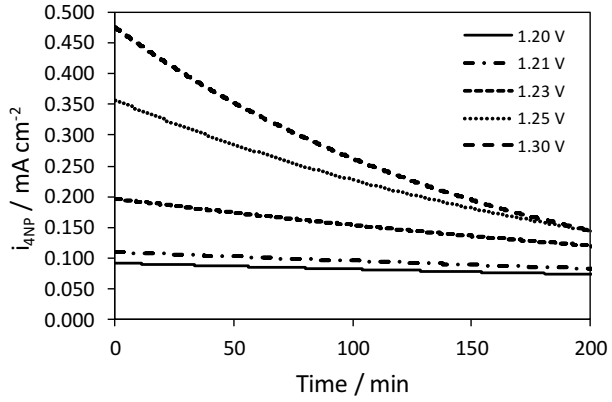

Fig. 6 Calculated current density of 4-NP oxidation (i_{4NP}) as a function of time at potentials between 1.2 and 1.3 V vs SCE. Above 1.3 V, as the reaction rate becomes limited mass transport, the 4-NP oxidation current densities become the same

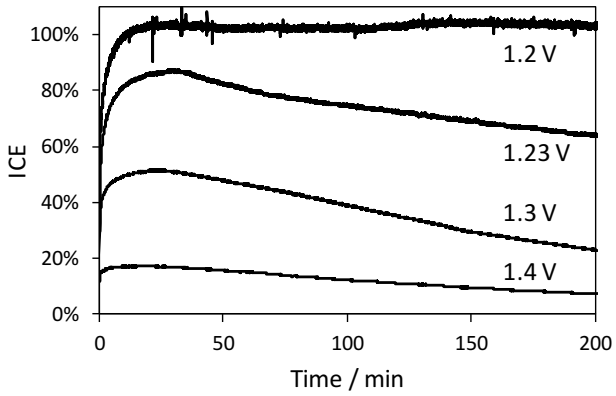

Fig. 7 Instantaneous current efficiency over time as function of anode potential

rate. Secondly, it is clear that even under conditions where mass transport does not limit the oxidation rate, the OER can still consume a significant proportion of the supplied current. Under these conditions, to improve the energy efficiency of electrochemical wastewater treatment, the anodes must promote organic oxidation over the OER. Hence, to obtain more efficient anode for organic oxidation, anode material should have the following characteristics:

- Capable of generating adsorbed hydroxyl radical fast enough at which high coverage of higher oxide (S-O) on the anode surface is obtained.
- The electrocatalytic of anode material should be in favour of fast reaction to organic oxidation or very slow for oxygen evolution reaction
- The anode coating structure should provide high active surface area, this leads to increase in the electrocatalytic performance of the anode.

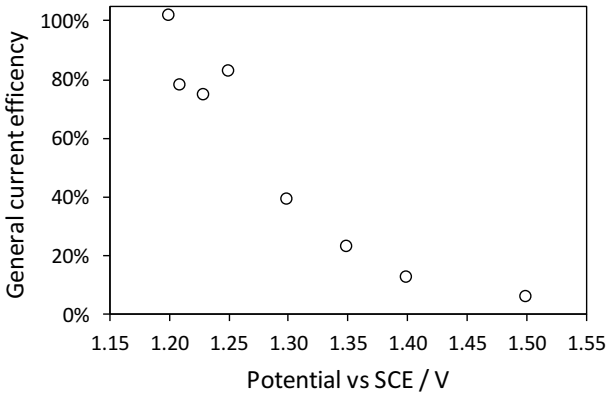

Fig. 8 General current efficiency over 200 min of oxidation as a function of anode potential

4 Conclusions

In this study, the inherent kinetics of the 4-NP oxidation reaction at IrO_2-Sb_2O_5-SnO_2/Ti anode have been investigated. It has been shown that potential dependence of the pseudo first order oxidation rate constant is consistent with potential dependence of the S-O surface coverage, which strongly suggests that this anode follows the "active" anode mechanism. The potential range where the oxidation is limited by reaction kinetics is quite narrow (1.2-1.3 V), with the oxidation rate of 4-NP becoming limited by mass transport above 1.3 V. For anodes following the "active" anode mechanism, operating below the mass transport limiting conditions is critical to maximising the ICE for the process. Contrary to the common assumption that the organic oxidation reaction will be much faster than the OER in absence of mass transport limitations, we find that this is only true at low overpotentials and thus conclude that determining the ICE under the expected process conditions is important. By using a simple reaction model, our analysis shows that the evaluation of the ICE by using a measured rate constant is a useful method to understand the performance of electrochemical wastewater oxidation. Specifically we show that it is possible to directly calculate the current going to 4-NP oxidation compared with the OER and thus the instantaneous and general current efficiencies can be determined as a function of time and potential. The most efficient wastewater oxidation process is when the anode potential is as low as possible due to the differences in dependences of the OER and 4-NP oxidation rate on the S-O surface coverage. Thus it must be concluded that to improve the efficiency of electrochemical wastewater oxidation processes, the anode materials should have at high coverage of adsorbed oxygen at low potentials. It should also be noted that by operating at low anode potentials, the processes energy efficiency will also be increased due to the smaller cell potentials which would be required. While low anode potentials will improve current and energy efficiency, the net rate of 4-NP oxidation is low and thus

a compromise between higher net oxidation rates and process efficiency may be required if such a process was to be implemented in an industrial setting.

References

1. R. Andreozzi, V. Caprio, A. Insola, and R. Marotta. Advanced oxidation processes (AOP) for water purification and recovery. *Catalysis Today*, 53(1):51–59, 1999.
2. S. Parsons. *Advanced oxidation processes for water and wastewater treatment*. IWA, London, 2004.
3. A. Sonune and R. Ghate. Developments in wastewater treatment methods. *Desalination*, 167:55–63, 2004.
4. R. Helmer and I. Hespanhol. *Water pollution control : a guide to the use of water quality management principles*. E&FN Spon, London ; New York, 1st. edition, 1997.
5. C. Comninellis, A. Kapalka, S. Malato, S. A. Parsons, L. Poulios, and D. Mantzavinos. Advanced oxidation processes for water treatment: advances and trends for R&D. *Journal of Chemical Technology and Biotechnology*, 83(6):769–776, 2008.
6. I. Sires, E. Brillas, M. A. Oturan, M. A. Rodrigo, and M. Panizza. Electrochemical advanced oxidation processes: today and tomorrow. A review. *Environmental Science and Pollution Research*, 21(14):8336–8367, 2014.
7. M. A. Oturan and J. J. Aaron. Advanced Oxidation Processes in Water/Wastewater Treatment: Principles and Applications. A Review. *Critical Reviews in Environmental Science and Technology*, 44(23):2577–2641, 2014.
8. O. J. Murphy, G. D. Hitchens, L. Kaba, and C. E. Verostko. Direct Electrochemical Oxidation of Organics for Waste-Water Treatment. *Water Research*, 26(4):443–451, 1992.
9. C. Comninellis. Electrocatalysis in the electrochemical conversion/combustion of organic pollutants for waste water treatment. *Electrochimica Acta*, 39(1112):1857–1862, 1994.
10. M. Panizza and G. Cerisola. Direct And Mediated Anodic Oxidation of Organic Pollutants. *Chemical Reviews*, 109(12):6541–6569, 2009.
11. C. A. Martínez-Huitle and S. Ferro. Electrochemical oxidation of organic pollutants for the wastewater treatment: direct and indirect processes. *Chemical Society Reviews*, 35(12):1324–1340, 2006.
12. Á. Anglada, A. Urtiaga, and I. Ortiz. Contributions of electrochemical oxidation to waste-water treatment: fundamentals and review of applications. *Journal of Chemical Technology and Biotechnology*, 84(12):1747–1755, 2009.
13. B. Adams, M. Tian, and A. Chen. Design and electrochemical study of SnO_2-based mixed oxide electrodes. *Electrochimica Acta*, 54(5):1491–1498, 2009.
14. B. J. Hernlem. Electrolytic destruction of urea in dilute chloride solution using DSA electrodes in a recycled batch cell. *Water Research*, 39(11):2245–2252, 2005.
15. C. A. Martínez-Huitle, S. Ferro, and A. De Battisti. Electrochemical incineration of oxalic acid - Role of electrode material. *Electrochimica Acta*, 49(22-23):4027–4034, 2004.
16. M. Panizza, P. A. Michaud, G. Cerisola, and C. Comninellis. Anodic oxidation of 2-naphthol at boron-doped diamond electrodes. *Journal of Electroanalytical Chemistry*, 507(1-2):206–214, 2001.
17. A.M. Polcaro, A. Vacca, S. Palmas, and M. Mascia. Electrochemical treatment of wastewater containing phenolic compounds: oxidation at boron-doped diamond electrodes. *Journal of Applied Electrochemistry*, 33(10):885–892, 2003.
18. A. M. Polcaro, M. Mascia, S. Palmas, and A. Vacca. Electrochemical degradation of diuron and dichloroaniline at BDD electrode. *Electrochimica Acta*, 49(4):649–656, 2004.
19. O. Simond and C. Comninellis. Anodic oxidation of organics on Ti/IrO_2 anodes using Nafion as electrolyte. *Electrochimica Acta*, 42(1314):2013–2018, 1997.
20. M. Tian, L. Bakovic, and A. C. Chen. Kinetics of the electrochemical oxidation of 2-nitrophenol and 4-nitrophenol studied by in situ UV spectroscopy and chemometrics. *Electrochimica Acta*, 52(23):6517–6524, 2007.

21. P. Cañizares, C. Saez, J. Lobato, and M. A. Rodrigo. Electrochemical Treatment of 4-Nitrophenol-Containing Aqueous Wastes Using Boron-Doped Diamond Anodes. *Industrial & Engineering Chemistry Research*, 43(9):1944–1951, 2004.
22. L. S. Andrade, T. T. Tasso, D. L. da Silva, R. C. Rocha, N. Bocchi, and S. R. Biaggio. On the performances of lead dioxide and boron-doped diamond electrodes in the anodic oxidation of simulated wastewater containing the Reactive Orange 16 dye. *Electrochimica Acta*, 54(7):2024–2030, 2009.
23. C. Bock and B. MacDougall. The electrochemical oxidation of organics using tungsten oxide based electrodes. *Electrochimica Acta*, 47(20):3361–3373, 2002.
24. F. Bonfatti, S. Ferro, F. Lavezzo, M. Malacarne, G. Lodi, and A. De Battisti. Electrochemical incineration of glucose as a model organic substrate - II. Role of active chlorine mediation. *Journal of the Electrochemical Society*, 147(2):592–596, 2000.
25. S. Fierro, L. Ouattara, E. H. Calderon, E. Passas-Lagos, H. Baltruschat, and C. Comninellis. Investigation of formic acid oxidation on Ti/IrO_2 electrodes. *Electrochimica Acta*, 54(7):2053–2061, 2009.
26. R. J. Watts, M. S. Wyeth, D. D. Finn, and A. L. Teel. Optimization of Ti/SnO_2-Sb_2O_5 anode preparation for electrochemical oxidation of organic contaminants in water and wastewater. *Journal of Applied Electrochemistry*, 38(1):31–37, 2008.
27. P. Cañizares, J. García-Gómez, J. Lobato, and M. A. Rodrigo. Modeling of Wastewater Electro-oxidation Processes Part I. General Description and Application to Inactive Electrodes. *Industrial & Engineering Chemistry Research*, 43(9):1915–1922, 2004.
28. M. Mascia, A. Vacca, S. Palmas, and A. M. Polcaro. Kinetics of the electrochemical oxidation of organic compounds at BDD anodes: modelling of surface reactions. *Journal of Applied Electrochemistry*, 37(1):71–76, 2007.
29. O. Simond, V. Schaller, and C. Comninellis. Theoretical model for the anodic oxidation of organics on metal oxide electrodes. *Electrochimica Acta*, 42(13-14):2009–2012, 1997.
30. P. Cañizares, J. García-Gómez, J. Lobato, and M. A. Rodrigo. Modeling of Wastewater Electro-oxidation Processes Part II. Application to Active Electrodes. *Industrial & Engineering Chemistry Research*, 43(9):1923–1931, 2004.
31. O. Scialdone. Electrochemical oxidation of organic pollutants in water at metal oxide electrodes: A simple theoretical model including direct and indirect oxidation processes at the anodic surface. *Electrochimica Acta*, 54(26):6140–6147, 2009.
32. M. A. Rodrigo, P. A. Michaud, I. Duo, M. Panizza, G. Cerisola, and C. Comninellis. Oxidation of 4-chlorophenol at boron-doped diamond electrode for wastewater treatment. *Journal of the Electrochemical Society*, 148(5):D60–D64, 2001.
33. H. B. Beer. The Invention and Industrial-Development of Metal Anodes. *Journal of the Electrochemical Society*, 127(8):C303–C307, 1980.
34. A. F. Gil, L. Galicia, and I. Gonzalez. Diffusion coefficients and electrode kinetic parameters of different Fe(III)-sulfate complexes. *Journal of Electroanalytical Chemistry*, 417(1-2):129–134, 1996.
35. U. K. Klaning, K. Sehested, and J. Holcman. Standard Gibbs energy of formation of the hydroxyl radical in aqueous solution. Rate constants for the reaction $ClO_2^- + O_3 \rightleftharpoons O_3^- + ClO_2$. *The Journal of Physical Chemistry*, 89(5):760–763, 1985.
36. C. De Pauli and S. Trasatti. Composite materials for electrocatalysis of O_2 evolution: $IrO_2 + SnO_2$ in acid solution. *Journal of Electroanalytical Chemistry*, 538-539:145–151, 2002.
37. J. O'M. Bockris. Kinetics of Activation Controlled Consecutive Electrochemical Reactions: Anodic Evolution of Oxygen. *The Journal of Chemical Physics*, 24(4):817–827, 1956.
38. C. De Pauli and S. Trasatti. Electrochemical Surafce Characterization of $IrO_2 + SnO_2$ Mixed Oxide Electrodes. *Journal of Electroanalytical Chemistry*, 396:161–168, 1995.
39. A. T. Marshall and L. Vaisson-Béthune. Avoid the quasi-equilibrium assumption when evaluating the electrocatalytic oxygen evolution reaction mechanism by Tafel slope analysis. *Electrochemistry Communications*, 61:23–26, 2015.
40. E. Gileadi. Problems in interfacial electrochemistry that have been swept under the carpet. *Journal of Solid State Electrochemistry*, 15(7-8):1359–1371, 2011.
41. R. Niesner and A. Heintz. Diffusion coefficients of aromatics in aqueous solution. *Journal of Chemical and Engineering Data*, 45(6):1121–1124, 2000.

42. A. Kapalka, G. Foti, and C. Comninellis. Kinetic modelling of the electrochemical mineralization of organic pollutants for wastewater treatment. *Journal of Applied Electrochemistry*, 38(1):7–16, 2008.
43. J. Lea and A. A. Adesina. Oxidative degradation of 4-nitrophenol in UV-illuminated titania suspension. *Journal of Chemical Technology and Biotechnology*, 76(8):803–810, 2001.
44. S. Chaliha, K. G. Bhattacharyya, and P. Paul. Oxidation of 4-nitrophenol in water over Fe(III), Co(II), and Ni(II) impregnated MCM41 catalysts. *Journal of Chemical Technology and Biotechnology*, 83(10):1353–1363, 2008.
45. J. Cornard, Rasmiwetti, and J. Merlin. Molecular structure and spectroscopic properties of 4-nitrocatechol at different pH: UVvisible, Raman, DFT and TD-DFT calculations. *Chemical Physics*, 309(23):239–249, 2005.
46. Sirajuddin, M. I. Bhanger, A. Niaz, A. Shah, and A. Rauf. Ultra-trace level determination of hydroquinone in waste photographic solutions by UVvis spectrophotometry. *Talanta*, 72(2):546–553, 2007.
47. M. A. Oturan, J. Peiroten, P. Chartrin, and A. J. Acher. Complete Destruction of p-Nitrophenol in Aqueous Medium by Electro-Fenton Method. *Environmental Science & Technology*, 34(16):3474–3479, 2000.